Far field acoustic response of a
co-rotating vortex pair

Keith LIOW, Mark THOMPSON and Kerry HOURIGAN

Department of Mechanical Engineering
Monash University, Clayton, Victoria, AUSTRALIA

ABSTRACT

Powell's (1964) acoustic analogy is used to model the far field acoustic response due to the leap frogging motion of a co-rotating vortex pair. A two step approach is adopted where the time dependent incompressible flow is first modelled followed by an aeroacoustic computation of the far field acoustic fluctuations. Numerical results are compared with the analytical solutions from the method of matched asymptotic expansions and direct numerical simulation. It is found to be important to model the initial condition by a ramping function to suppress non-physical acoustic transients.

1. INTRODUCTION

Studies of the far field acoustic signature of a compact flow field is of vital importance in efforts to understand subsonic jet noise generation and subsequently to apply active noise control techniques. Several acoustic analogies have been developed to model acoustical fluctuations from low Mach number flows. Lighthill (1952) has proposed an acoustic model with the source derived *a priori* from the fluctuating Reynolds' stresses. Powell's (1964) acoustic model is based on a source region of non-vanishing vorticity. Theoretical investigations of acoustic analogies have often been limited to inviscid point vortices (Powell (1964), Müller and Obermeier (1967), Yates (1978)). The aim of this paper is to present the authors' development of the numerical application of Powell's acoustic model.

1.1 FLOW DESCRIPTION

The two vortex cores of equal circulation are initially positioned with a center to center spacing of $2R$. The vortex-induced flow rotates with a co-rotation Mach number $(\omega R)/c$. The Gaussian vorticity distribution of the vortex core is based on Mitchell's *et al.* (1995) paper. Each vortex core has zero radial velocity component. The vorticity and tangential velocity of each core are defined as follows :

$$\zeta = 3.57 \frac{U_o}{R_o} \exp(-1.25(\frac{r}{R_o})^2), \tag{1}$$

$$V = (3.57 U_o R_o) \frac{1 - \exp(-1.25(\frac{r}{R_o})^2)}{1.25 r}, \tag{2}$$

where the circulation of the flow is $\Gamma_o = 2\pi U_o R_o / 0.7$ and ω_i is the angular rate of rotation based on the initial velocity field. Figure 1 depicts these distributions as a function of distance.

1.2 ACOUSTIC MODEL

Powell's (1964) theory of vortex sound uses the far field pressure, p, as the fundamental acoustic variable and defines the source from the Coriolis acceleration, $(\zeta \times \mathbf{V})$.

$$\frac{\partial^2 p}{\partial t^2} - c_o^2 \nabla^2 p = \rho_o (\nabla \cdot (\zeta \times \mathbf{V})), \tag{3}$$

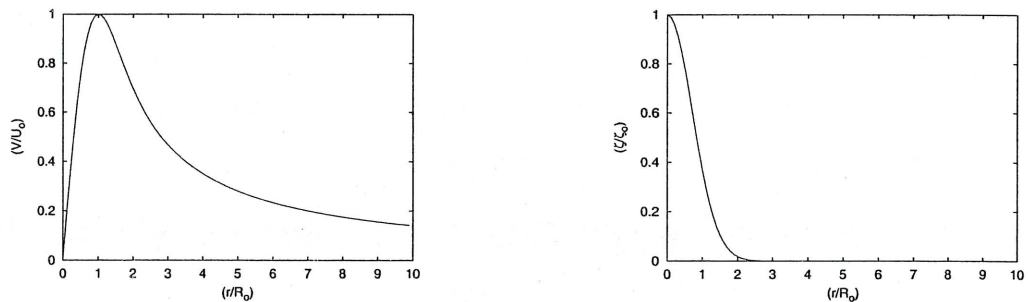where c_o, ρ_o represent ambient values of the acoustic medium.

Figure 1: Vortex core tangential velocity and vorticity profile against normalised distance.

Müller and Obermeier (1967) used the method of matched asymptotic expansion (MAE) and derived the analytical far field acoustic solution from a spinning pair of inviscid point vortices. The analytical pressure contours show a double spiral behaviour described by

$$p(r, \theta, t) = -\frac{\rho_o \Gamma^4}{64\pi^3 R_o^4 c_o^2}(J_2(kr)\sin(2\theta - 2\Omega t) + Y_2(kr)\cos(2\theta - 2\Omega t)), \qquad (4)$$

where k is the wavenumber, Ω is the angular rate of rotation for an inviscid co rotating point vortex pair. J_2 and Y_2 are second order Bessel functions of the first and second kind respectively.

2. NUMERICAL METHOD

The two dimensional unsteady incompressible Navier-Stokes equations are solved numerically using a commercial finite volume CFD software package (Fluent Inc.). Spatial convective terms are discretised using QUICK interpolation scheme. The SIMPLE algorithm is used in pressure-velocity coupling. The unsteady flow field is marched in time using a second order accurate implicit time-stepping scheme. The flow is initialised with the velocity field of the co rotating vortex pair. The initial hydrodynamic pressure field is obtained by solving the Poisson equation for pressure. The computational domain, L_{CFD} extends to $30R$ in the x, y directions. At the boundaries, u, v are based on the asymptotic far field solution of the inviscid co rotating vortex pair.

Spatial accuracy of the CFD modelling is studied by monitoring of dissipation of flow vorticity with different values of $(\Delta x_{CFD}/R_o) = 0.125, 0.1428, 0.167$. Temporal resolution studies to minimise numerical damping were also conducted with $\Delta t_{CFD} = 0.4, 0.2, 0.1, 0.05$s.

The aeroacoustic computations are performed using a seven point stencil central difference scheme which is sixth order accurate in space. At the computational aeroacoustic (CAA) boundary, there are three ghost points. On ghost nodes where an axisymmetric stencil is not possible, a non-symmetric stencil was used. Temporal marching is advanced using fourth-order Runge-Kutta scheme. An exponential stretching function was used in the computational (CAA) domain. Non reflecting radiation boundary conditions based on Bayliss and Turkel (1980) are implemented on all the CAA boundaries.

The CAA domain, L_{CAA} extends to two wavelengths in the x, y directions. There are 25 grid points across the vortex core. Outgoing far field acoustic waves were adequately resolved by a minimum of 20 grid points across the entire wavelength. The choice of time step was dictated by the numerical stability of the computational scheme at $(c\Delta t_{CAA}/R) = 0.009167$. Grid stretching is introduced to resolve the near field acoustic source and the far field acoustic waves. An important consideration in grid stretching is the local maximum stretching values. The stretching function adopted was an exponential one. Mitchell et al. (1995) has reported on non-physical reflections as the initial acoustic transient traverses through the highly stretched region. The effects of grid stretching on the propagation of acoustic transients were examined with maximum local stretching at 7.4% and 3.99% (see figure 3). Further minimisation of the reflections is performed by adding artificial dissipation ($\mu_a = 0.01$). Excessive damping might be unfavourable and this issue is currently under investigation.

Past researchers modelling acoustic fluctuations from a co rotating vortex pair have indicated the occurence of a high frequency wave component in the far field followed by the progression of the acoustic waves (Lee and Koo (1995), Mitchell et al. (1995)). The likely cause is the erroneous initial condition from abrupt spinning of the vortex pair. To model the initial acoustic transients, a ramping function is introduced to artificially create the vortex cores. The vortex cores are ramped from zero circulation to full strength Γ_o. To achieve asmooth exponential ramping function, the control parameter ($\Delta t_{CAA}/T_{ramp}$) was set to 0.000625.
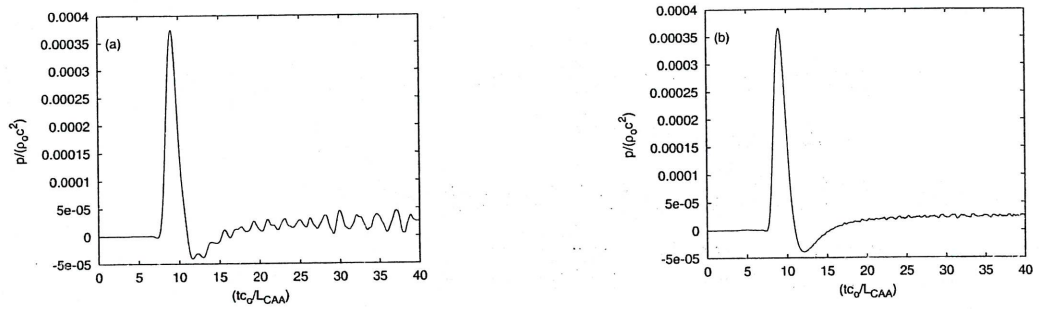
Figure 2: Trace of acoustic pressure during initial acoustic transient with maximum local stretching at 7.3% (2a), 3.9% (2b) with zero dissipation.
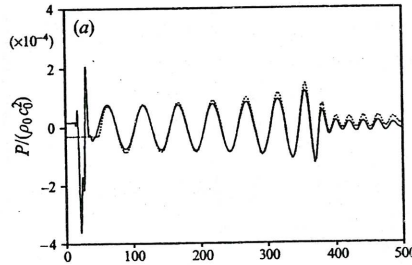

Figure 3: Far field trace of acoustic pressure at $r/\lambda = 2$ along positive x-axis of Mitchell's DNS results.

The hydrodynamic flow variables, (u, v, ζ) from the CFD domain are exported into the CAA domain using bilinear interpolation. Temporally, cubic spline interpolation was used to obtain intermediate values between the CFD time steps. A resolution study of two, four and six intervals was conducted and consequently no significant increase in accuracy was obtained beyond a six interval cubic spline interpolation.

3. RESULTS AND DISCUSSION

Results are presented for the modelling of the flow field and its far field acoustic effects. The Reynolds number of the flow field based on circulation of each vortex is Re $= \rho_\infty \Gamma / \mu = 7500$. The initial co-rotation Mach number, $M_{cr} = 0.06$.

Four complete co-rotations were evident before eventual merging into a single circular vortex core. The angular velocity was observed to increase as the vortex cores moved closer to conserve angular momentum. The vortex cores 'loses' its initial circular profile and assumes an elliptical shape after the first co rotation. The merging process commences after approximately four half revolutions.

A comparison of two different values of grid stretching is shown in figure 2 where the vortex cores are ramped up and held stationary. The initial acoustic transient was found to generate unphysical reflections as it traverses the CAA domain. Such reflections were found to be grid-induced errors and as such, are classified as numerical noise.

Eight cycles of far field acoustic pressure data were generated from the flow field. A far field observation position is placed at $x = \lambda/2$ along the positive x-axis. Temporal evolution of far field acoustic pressure traces are shown in figure 4. Numerical results are compared with Mitchell's DNS results (Figure 3). The initial wave represents the propagation of the acoustic transient and were observed to be less spatially sharp than Mitchell's result. Far field acoustic waves results agree reasonably well in amplitude and oscillation frequency. The acoustic pressure cycles showed a gradual increase in amplitude and angular rate of rotation prior to merging.

The time history of the far field acoustical fluctuations at $x = \lambda/2$ is sampled. The Fourier component of the signal is obtained using a fast Fourier transform algorithm. The power spectral density in dB $(20\log(p/p_{ref}))$ is obtained by squaring both the real and imaginary components of the transform. Power spectral density obtained using the MAE reveals a singular fundamental frequency of the leading quadrupole term (figure 5). Comparison of analytical MAE results with numerical results reveal a higher frequency for the case of viscous co rotating vortex pair. However, acoustic power output agrees reasonably well.
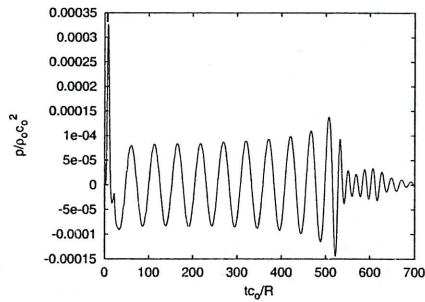
Figure 4: Far field trace of acoustic pressure at $r/\lambda = 2$ along positive x-axis.
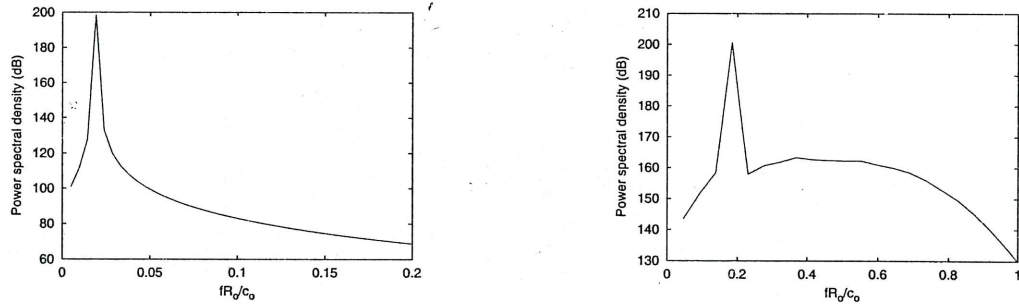

Figure 5: Power spectral density of acoustic pressure at $x = \lambda/2$ along positive x axis using MAE and numerical data. Note $p_{ref} = 2.0$mPa.

4. CONCLUSION

The computational coupling of CFD and CAA to solve aeracoustic problems is demonstrated. Accurate modelling of the far field acoustic effects of compact low Mach number flow fields involves appropriate modelling of the initial transient. Numerical parameters such as grid stretching and dissipation or filtering schemes must be optimised in modelling the growth and propagation of acoustic transients. Ongoing studies by the authors on quantifying and controlling the levels of reflections of initial acoustic transients will be published at a later date.

5. REFERENCES

BAYLISS, A. and TURKEL, E., "Far field boundary conditions for compressible flows", *J. Comp. Physics*, **48**, 182-199, 1982.

LEE, D.J. and KOO, S.O., "Numerical study of sound generation due to a spinning vortex pair", *AIAA Journal*, **33**, 20-26, 1995.

LIGHTHILL, M.J., "On sound generated aerodynamically", *Proc. R. Soc. Lond.*, **A211**, 564-587, 1952.

MÜLLER, E.A. and OBERMEIER, F., "The spinning vortices as a source of sound", *AGARD*, **CP-22**, 22.1-22.8, 1967.

MITCHELL, B.E., LELE, S.K. and MOIN, P., "Direct computation of the sound from a compressible co-rotating vortex pair", *J. Fluid Mech.*, **285**, 181-202, 1995.

POWELL, A., "Theory of vortex sound", *J. Acoust. Soc. Am.*, **36**, 177-195, 1964.

YATES, J.E., "Application of the Bernoulli enthalpy concept to the study of vortex noise and jet impingement noise", *NASA Contractor Rep.*, **2987**, 1978.